





Activation of Wnt/ β -catenin pathway mitigates blood–brain barrier dysfunction in Alzheimer’s disease

Qi Wang,^{1,2,†} Xiaomin Huang,^{1,†} Yixun Su,^{1,2} Guowei Yin,¹ Shouyu Wang,² Bin Yu,² Hui Li,^{1,2} Junhua Qi,¹  Hui Chen,³ Wen Zeng,⁴ Kai Zhang,⁵ Alexei Verkhratsky,^{6,7} Jianqin Niu² and  Chenju Yi¹

[†]These authors contributed equally to this work.

Alzheimer’s disease is a neurodegenerative disorder that causes age-dependent neurological and cognitive declines. The treatments for Alzheimer’s disease pose a significant challenge, because the mechanisms of disease are not being fully understood. Malfunction of the blood–brain barrier is increasingly recognized as a major contributor to the pathophysiology of Alzheimer’s disease, especially at the early stages of the disease. However, the underlying mechanisms remain poorly characterized, while few molecules can directly target and improve blood–brain barrier function in the context of Alzheimer’s disease. Here, we showed dysfunctional blood–brain barrier in patients with Alzheimer’s disease reflected by perivascular accumulation of blood-derived fibrinogen in the hippocampus and cortex, accompanied by decreased tight junction proteins Claudin-5 and glucose transporter Glut-1 in the brain endothelial cells. In the APP_{swe}/PS1_{dE9} (APP/PS1) mouse model of Alzheimer’s disease, blood–brain barrier dysfunction started at 4 months of age and became severe at 9 months of age. In the cerebral microvessels of APP/PS1 mice and amyloid- β -treated brain endothelial cells, we found suppressed Wnt/ β -catenin signalling triggered by an increase of GSK3 β activation, but not an inhibition of the AKT pathway or switching to the Wnt/planar cell polarity pathway. Furthermore, using our newly developed optogenetic tool for controlled regulation of LRP6 (upstream regulator of the Wnt signalling) to activate Wnt/ β -catenin pathway, blood–brain barrier malfunction was restored by preventing amyloid- β -induced brain endothelial cells impairments and promoting the barrier repair. In conclusion, targeting LRP6 in the Wnt/ β -catenin pathway in the brain endothelium can alleviate blood–brain barrier malfunction induced by amyloid- β , which may be a potential treatment strategy for Alzheimer’s disease.

- 1 Research Centre, The Seventh Affiliated Hospital of Sun Yat-sen University, Shenzhen, China
- 2 Department of Histology and Embryology, Chongqing Key Laboratory of Neurobiology, Brain and Intelligence Research Key Laboratory of Chongqing Education Commission, Third Military Medical University, Chongqing, China
- 3 School of Life Sciences, University of Technology Sydney, Sydney 2007, Australia
- 4 Department of Cell Biology, State Key Laboratory of Trauma, Burn and Combined Injury, Third Military Medical University, Chongqing, China
- 5 Department of Biochemistry, School of Molecular and Cellular Biology, the University of Illinois at Urbana-Champaign, Urbana, IL 61801, USA
- 6 Faculty of Biology, Medicine and Health, The University of Manchester, Manchester, UK
- 7 Achucarro Center for Neuroscience, IKERBASQUE, Basque Foundation for Science, 48011 Bilbao, Spain

Received January 11, 2022. Revised May 29, 2022. Accepted June 14, 2022. Advance access publication July 5, 2022

© The Author(s) 2022. Published by Oxford University Press on behalf of the Guarantors of Brain.

This is an Open Access article distributed under the terms of the Creative Commons Attribution-NonCommercial License (<https://creativecommons.org/licenses/by-nc/4.0/>), which permits non-commercial re-use, distribution, and reproduction in any medium, provided the original work is properly cited. For commercial re-use, please contact journals.permissions@oup.com

Correspondence to: Chenju Yi
Research Centre, The Seventh Affiliated Hospital of Sun Yat-sen University
Shenzhen 518107, China
E-mail: yichj@mail.sysu.edu.cn

Correspondence may also be addressed to: Jianqin Niu
Department of Histology and Embryology
Chongqing Key Laboratory of Neurobiology
Brain and Intelligence Research Key Laboratory of Chongqing Education Commission
Third Military Medical University
Chongqing 400038, China
E-mail: jianqinniu@163.com

Alexei Verkhratsky
Faculty of Biology, Medicine and Health
The University of Manchester, Manchester, UK
E-mail: alexei.verkhratsky@manchester.ac.uk

Keywords: blood–brain barrier; opsin-free optogenetics; LRP6; A β ; endothelial cells

Abbreviations: APP/PS1 = APP_{swe}/PS1_{dE9}; BBB = blood–brain barrier; BEC = brain endothelial cells; GSK3 β = glycogen synthase kinase 3 β ; PCP = planar cell polarity; Zo-1 = zonula occludens-1

Introduction

Alzheimer's disease is a neurodegenerative disorder that causes age-dependent neurological and cognitive decline. Despite ongoing efforts, the current understanding of Alzheimer's disease pathophysiology^{1–5} failed to guide to the development of drugs capable of arresting or reversing the disease progression.^{6,7} Recent studies have highlighted the dysfunction of the blood–brain barrier (BBB) as an early event of Alzheimer's disease,^{8–12} whereas manipulations with BBB may provide a new target for intervention.

Tight and adherens junction proteins connect adjacent brain endothelial cells (BECs) to seal the BBB, which is composed of endothelial and parenchymal basement membranes, pericytes and astrocytic endfeet.^{13,14} Selective permeability of the BBB restricts the passage of pathogens, and regulates the transport of essential nutrients and metabolites.¹⁵ The impairments of BBB structural components and BECs in particular, compromise the integrity and function of BBB.¹⁶ Pathological changes in BECs are often reflect dysregulation of tight junctions,¹⁷ including changes in expression of the tight junction protein Claudin-5,¹⁸ and the tight junction-actin cytoskeleton connecting protein zonula occludens-1 (Zo-1).¹⁹ In a mouse model of Alzheimer's disease, reduced expression of glucose transporter Glut-1 in the BECs impaired tight junction integrity and BBB function, leading to cerebral microvascular degeneration.²⁰ However, the contribution of BBB dysfunction to Alzheimer's disease pathogenesis has not been widely acknowledged. A recent study using dynamic contrast-enhanced MRI also found increased BBB permeability in Alzheimer's disease brains.⁸ This increase in permeability may result in increased levels of albumin, haemoglobin-derived peptides and prothrombin found in the perivascular brain tissues of patients with Alzheimer's disease,^{21–23} although some studies found no significant increase in the extravascular levels of fibrinogen, prealbumin or immunoglobulins.^{24,25}

Wnt signalling is critical for the development of BECs.²⁶ This signalling cascade involves canonical Wnt/ β -catenin pathway, non-

canonical Wnt/ Ca^{2+} pathway and Wnt/planar cell polarity (PCP) pathway.²⁷ Tight junction proteins and Glut-1 are the transcriptional targets of Wnt/ β -catenin pathway in BECs,^{26,28,29} while the integrity of endothelial tight junctions is regulated by the Wnt/PCP pathway.³⁰ The Wnt signalling is significantly reduced in various cell types in the Alzheimer's disease brains.^{31,32} Which Wnt pathway is specifically involved in the BECs dysfunction in Alzheimer's disease pathology remains, however, unknown.

Extracellular amyloid β -protein (A β) and its isoforms were shown to regulate Wnt signalling.^{32–35} For example, fibrillar A β ³⁴ or A β oligomer³⁵ can suppress the Wnt/ β -catenin pathway in the neurons by binding to the Frizzled receptor of Wnt ligands. In other cell types, A β oligomers reduce AKT activation by increasing the inhibitory regulation of glycogen synthase kinase 3 β (GSK3 β), with subsequent suppression of the Wnt/ β -catenin pathway.^{36,37} At the synaptic level, A β -induced dickkopf-1 (Dkk1) expression switches from the Wnt/ β -catenin pathway to the Wnt/PCP pathway by degrading the Wnt/ β -catenin pathway coreceptor LDL Receptor Related Protein 6 (LRP6).^{32,38,39} The A β precursor protein (APP) interacts with Vang-like 2 protein (Vangl2) to specifically activate the Wnt/PCP pathway, which drives synapse retraction.³² Therefore, we aimed to investigate how the Wnt pathway in the BECs is affected at the early stages of Alzheimer's disease, and whether this pathway is a plausible target for intervention.

In this study, we firstly demonstrated BBB dysfunction and BEC disruption in post-mortem human Alzheimer's disease brains. Then in APP_{swe}/PS1_{dE9} (APP/PS1) mouse model of Alzheimer's disease, we showed that BBB dysfunction and BEC impairments started at 4 months of age and progressed with ageing. In BECs *in vitro*, we found that the A β oligomer suppressed the Wnt/ β -catenin signalling through the activation of GSK3 β , but not through the inhibition of AKT pathway or switching to the Wnt/PCP pathway. Last, we provided the evidence that activating Wnt/ β -catenin pathway in BECs by targeting its upstream regulator LRP6 can restore A β oligomer-induced pathologies, making LRP6 a promising new target for Alzheimer's disease drug development.

Materials and methods

Immunohistochemistry for human brain samples

Human post-mortem brain specimens were obtained from the Chinese brain bank centre under the ethical approval by the Ethics Committee of the Brain Bank. The brain specimens were identified as Alzheimer's disease by the Brain Bank using the ABC method of Alzheimer's disease neuropathologic change, which were categorized into four levels 'Not, Low, Intermediate, High' as shown in [Supplementary Table 1](#). After deparaffinization, the paraffin-embedded sections were treated with 3% H₂O₂ and processed for antigen retrieval. The sections were blocked with blocking solution and incubated with targeted primary antibody for 2 h at 37°C and overnight at 4°C. After reaction with biotin-specific secondary antibody and signal enhanced by SABC or SABC-AP (Boster) on the following day, the sections were processed with DAB Substrate Kit (Abcam) and BCIP/NBT kit (Boster) for immunoreactive signals detection. The stained sections were dehydrated, mounted in neutral balsam, then examined with a bright field microscope and analysed by Fuji software. Primary antibodies included: A β (1:500, mouse, 800701, BioLegend), CD31 (1:50, rabbit, ab28346, Abcam), Fibrinogen (1:300, mouse, ab58207, Abcam), Cldn5 (1:20, rabbit, 35-2500, Invitrogen), Glut1 (1:100, rabbit, MA5-31960, Invitrogen) and Sox17 (1:100, goat, AF1924, R&D). For the quantification, we randomly selected six non-overlapping areas of 1 mm² in the cortex and hippocampus, respectively. Fiji software was used to quantify the fluorescent intensity in each image; then these intensities were averaged for each human brain. Finally, the fluorescent intensities were normalized to the healthy controls. The detailed information about healthy controls and Alzheimer's disease patients is listed in [Supplementary Table 1](#).

Animals

C57BL/6J (wild-type) mice and transgenic APP/PS1 mice were obtained from Nanjing Junke Bioengineering Co., Ltd, China. Male and female Sprague-Dawley rats of 10 days old were obtained from the animal centre of Army Medical University, China. All animals used in the study were maintained in a specific-pathogen-free animal facility. All procedures were performed under the ethical approval of the Sun Yat-Sen University Institutional Animal Care and Use Committee.

Immunofluorescence staining

Under deep anaesthesia, wild-type and APP/PS1 mice were perfused intracardially with cold PBS and 4% paraformaldehyde. The brains were removed, dehydrated, embedded in OCT media and snap-frozen. Cryostat sections (20 μ m) were preincubated with blocking buffer (PBS containing 2% BSA and 0.5% Triton-X100) for 30 min. For immunofluorescence staining, BECs on coverslips were fixed with 4% paraformaldehyde for 15 min and were then permeabilized and blocked with blocking buffer. Sections or coverslips were processed for immunostaining by overnight incubation at 4°C with primary antibodies, followed by Alexa Fluor conjugated secondary IgG antibodies for 1 h at room temperature. Then, the sections or coverslips were washed, mounted and examined with a confocal microscope. For the quantification of sections, five brain slices from each mouse brain were analysed. Fiji software was used to quantify the fluorescent intensity, which was averaged for each mouse and then normalized to wild-type group as relative change. For the quantification of coverslips, three independent

experiments with triplicates in each were performed. Five non-overlapping images from each coverslip were analysed. The values were calculated by fluorescence intensity standardized by DAPI positive cell number in each image by Fiji software, and then normalized to the control group to present the data as relative change and presented as a ratio. Primary antibody for immunofluorescence included: A β (1:200, rabbit, 36-6900, Invitrogen), CD31 (1:200, rat, 553370, BD), Fibrinogen (1:500, mouse, ab58207, Abcam), Cldn5 (1:100, rabbit, 35-2500, Invitrogen), Glut1 (1:200, rabbit, HPA031345, Sigma), CD13 (1:200, rabbit, ab108310, Abcam), IBA1 (1:1000, goat, ab5076, Abcam), GFAP (1:400, rabbit, ab7260, Abcam), Sox17 (1:200, goat, AF1924, R&D), Zo-1 (1:200, mouse, 339100, Invitrogen), Ki67 (1:1000, rabbit, 9129, CST) and Cleaved Caspase-3 (1:400, rabbit, 9661, CST).

Isolation of brain microvessels and primary BECs

The brain microvessels were isolated as previously described.²⁹ Briefly, the brains were collected and rinsed in ice-cold PBS, and the leptomeninges, cerebellum, brainstem and white matter were removed on ice. The remaining cortices were homogenized in 10 ml of DMEM containing 1 ml of 1 mg/ml collagenase (Sigma) and 0.1 mg/ml DNase I (Sigma), and shaken at 250 rpm for 1 h at 37°C. Then the homogenates were centrifuged at 1000g for 8 min at room temperature. The pellet was suspended in 25 ml of DMEM containing 20% BSA and centrifuged at 1000g for 20 min at room temperature. The pellet contained the brain microvessels for protein and RNA extraction. For primary BEC culture, the microvessels pellet was further homogenized in 5 ml DMEM containing 0.5 ml of 1 mg/ml collagenase-dispase (Roche) and 0.1 mg/ml DNase I, and shaken at 250 rpm for 30 min at 37°C. The cell pellet was then suspended in BEC culture medium and seeded on collagen-coated plates. Puromycin was supplied in the medium for the first 24 h to achieve high BEC purity.

Protein extraction and western blotting

To prepare protein lysates, tissues or cells were lysed in sodium dodecyl sulphate (SDS) lysis buffer supplemented with protease inhibitor cocktail and 2 mM phenylmethylsulphonyl fluoride (PMSF). Protein was quantified by Enhanced BCA Protein Assay Kit (Beyotime), and the normalized protein samples were denatured at 95°C for 10 min and separated by SDS-polyacrylamide gel electrophoresis. Membranes with transferred proteins were incubated with the primary antibodies overnight at 4°C followed by secondary antibodies, and detected with the Amersham ECL Prime Western Blotting Detection Reagent (GE Health) by ChampChemi 610 Chemiluminescence Imaging System (Beijing Sage Creation, China). For the quantifications, band densities were measured by Fiji software. The quantification of phosphorylated proteins was normalized to their total proteins. GAPDH was used as the housekeeping protein, and the data were presented as fold change to the control group. Primary antibodies for western blotting included: Cldn5 (1:1000, rabbit, AF5216, Affinity), Glut1 (1:1000, rabbit, ab115730, Abcam), Active β -catenin (1:1000, rabbit, 8814, CST), total β -catenin (1:1000, rabbit, 8480, CST), p-GSK3 β (1:1000, mouse, 14630, CST), total GSK3 β (1:1000, rabbit, 9315, CST), p-AKT (1:1000, rabbit, 13038, CST), total AKT (1:1000, rabbit, 4691, CST), p-VANGL2 (1:1000, rabbit, MA5-38241, Invitrogen), total VANGL2 (1:1000, rabbit, PA5-23207, Invitrogen), Cleaved Caspase-3 (1:1000, rabbit, 9661, CST), Caspase-3 (1:1000, rabbit, 9662, CST) and GAPDH (1:1000, mouse, AF0006, Beyotime).

RNA extraction and quantitative PCR with reverse transcription

Tissues or cells were washed with ice-cold PBS and then lysed directly by TRIzol (Thermo). Total RNA was isolated by RNeasy Plus Mini Kit (Qiagen), and reverse transcription was carried out using the Reverse Transcriptase kit (Takara), all according to the manufacturer's protocol. qPCR was carried out using FastStart Universal SYBR Green Master Mix (Roche) with Real-Time PCR Detection System (Roche). The relative expression of target genes was calculated using the $2^{-\Delta\Delta Ct}$ method normalized to the house-keeping gene *GAPDH*. The results are presented as a relative change compared to the controls.

Plasmid construction, lentivirus preparation and BEC infection

The plasmid vector was constructed as described previously.⁴⁰ The lentivirus was produced using third-generation lentiviral generation systems, the virus envelope plasmid, packaging plasmids and OptoLRP6, Δ CRY2 plasmids were transfected into 293T cell lines. Eight hours after transfection, the media were refreshed. The lentivirus-containing media was collected after 48 h culture and filtered with a 0.22 μ m filter. For BEC transfection, lentivirus was added into the culture medium at a multiplicity of infection of 20.

A β oligomer treatment of the primary BEC

Synthetic A β_{25-35} peptide (Sigma) was reconstituted in dimethyl sulphoxide (Sigma) and lyophilized overnight. The lyophilized peptide was either processed for oligomer formation or stored at -80°C for long-term storage. For oligomer formation, the lyophilized stock was resuspended in cell culture medium to the desired concentration and incubated at 37°C for 24 h to form the oligomers before the experiments. The validity of this method has been described previously.⁴¹ Before or after light stimulation, BEC was treated with A β_{25-35} at 20 μM . All assays were carried out 24 h after exposure to A β_{25-35} exposure. At least three independent experiments were performed.

TUNEL assay

Cell apoptosis was detected by TUNEL assay with the *In Situ* Cell Death Detection Kit (Roche) following the manufacturer's protocol. Cells were costained with DAPI then subjected to imaging.

Light stimulation

The instrument used for blue-light illumination was described previously.⁴² Briefly, the LED box was constructed by plugging blue LED lights into a breadboard containing a 12 cm \times 7 cm \times 3 cm aluminium box covered with a translucent plastic board. The LED lights were aligned with the centre of each well of the 12-well plate and were wired with resistors. The OptoLRP6-transfected or Δ CRY-transfected cells were illuminated on a 20 min on/40 min off cycle with blue light. The light intensity was adjusted to 25 lx at the level of the cells by adjusting the voltage.

In vitro trans-well permeability assay

Primary BECs were seeded on 24-well with a 0.4- μm pore polycarbonate membrane inserted trans-well plate. After receiving desired

treatment as described in each group, the cells were subjected to permeability assay. The upper chamber was filled with 150 μl of 1 mg/ml FITC-dextran (40 kDa), while the bottom plate well was replaced with 600 μl of fresh BEC culture media. Samples were collected from the bottom well at 30 min. Fluorescence intensities were measured with a microplate reader at 485 nm excitation and 535 nm emission wavelength. The data were compared and normalized to the control group.

Statistical analysis

The differences between two groups were analysed by a two-tailed Student's *t*-test. The differences between multiple groups were analysed by one-way ANOVA followed by Tukey *post hoc* tests (GraphPad Prism software). $P < 0.05$ was considered significant, indicated as * $P < 0.05$, ** $P < 0.01$. Unless otherwise specified, data were presented as mean \pm standard error of the mean (SEM).

Data availability

The raw data supporting the findings of this study will be made available by the corresponding authors, upon reasonable request.

Results

BBB dysfunction and BEC disruption in patients with Alzheimer's disease

Dysfunction of the BBB is not universally acknowledged in Alzheimer's disease, since there are inconsistencies among studies owing to the sensitivity of the methods.^{8,21–25,43–45} In this study, using optimized immunohistochemical double staining method, we investigated five post-mortem human Alzheimer's disease brains and age- and sex-matched healthy control brains (Supplementary Table 1). A β plaques were visible in the hippocampus and cortex of the Alzheimer's disease brains (Fig. 1A and B). Fibrinogen, a major blood protein, was detected in the Alzheimer's disease brain tissues being accumulated around microvessels (Fig. 1A and B), indicating a vascular leakage. The expression of tight junction protein Claudin-5 was significantly decreased by $40 \pm 13.6\%$ in the hippocampus and by $40.5 \pm 14.9\%$ in the cortex of Alzheimer's disease brains, respectively (both $P < 0.05$, versus control, Fig. 1C). The level of blood vessel colocalized Glut-1 was reduced by $31.8 \pm 10.9\%$ in both hippocampus and cortex of Alzheimer's disease brains (both $P < 0.05$, versus control, Fig. 1D), suggesting the BBB disruption and BEC dysfunction.⁴⁶ These findings are consistent with the pathological changes in BECs in previous studies.^{10,11,47,48}

BBB dysfunction and BEC disruption occur in the early stage of Alzheimer's disease in APP/PS1 mouse model

To assay the timing of BBB dysfunction and BEC malfunction in Alzheimer's disease, we used the APP/PS1 mouse model focusing on the hippocampus. We first examined BBB function in 2, 4 and 9-month-old APP/PS1 mice, representing A β amyloidosis at different stages (Supplementary Fig. 1). A β deposits started at 4 months of age and were significantly increased at 9 months (Fig. 2A).

Fibrinogen was used as a marker of BBB leakage. In wild-type controls, fibrinogen can only be detected within the vascular lumen, suggesting intact BBB (Fig. 2B and E). In 4-month-old

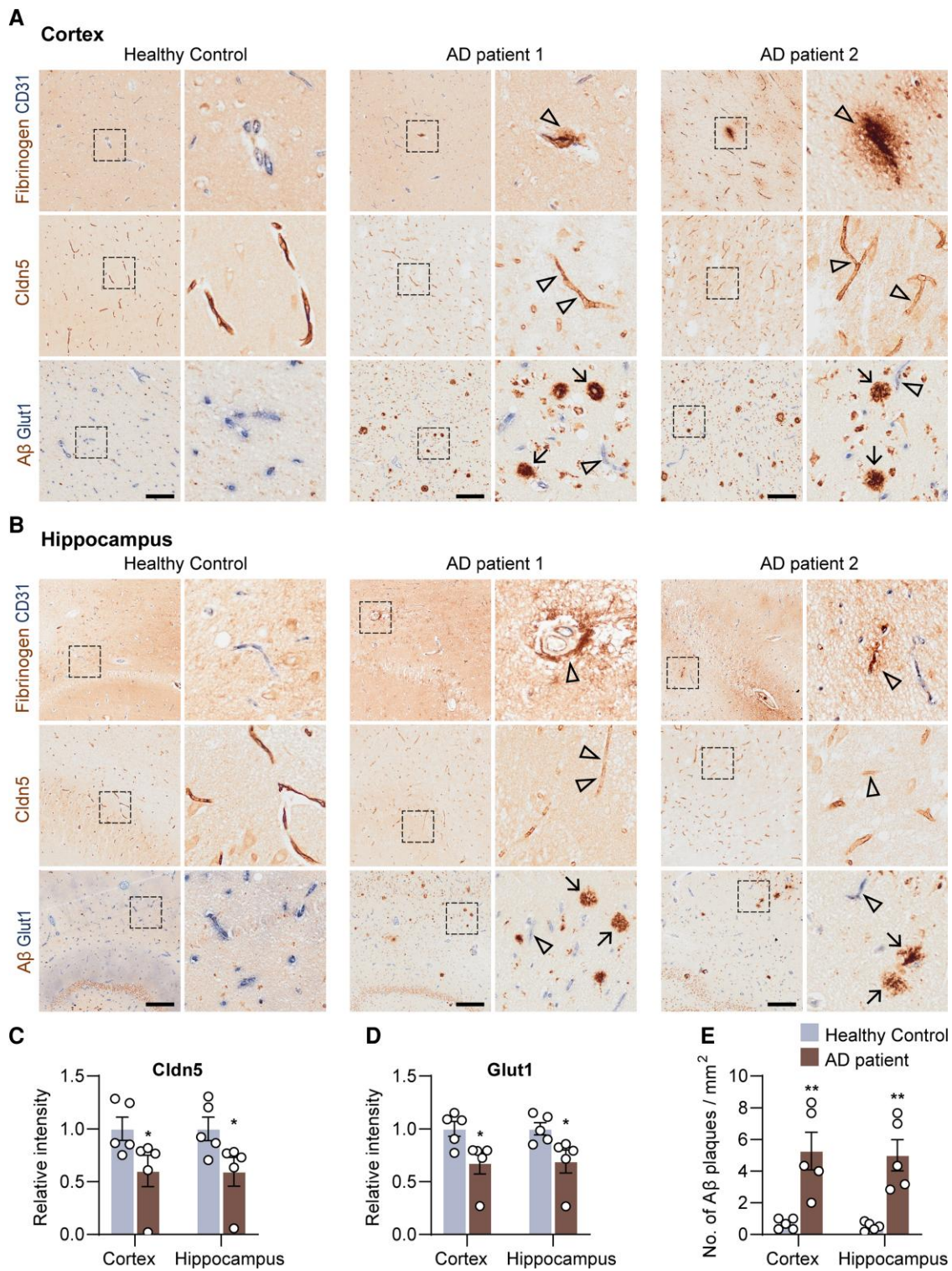


Figure 1 BBB dysfunction and BEC disruption in post-mortem Alzheimer's disease brains. (A) Fibrinogen/CD31, Cldn5 and Aβ/Glut1 staining in the cortex and (B) hippocampus of post-mortem health control and patients with Alzheimer's disease. (C) Quantification of Cldn5 and (D) Glut1 intensity, and (E) Aβ plaques in the cortex and hippocampus of healthy controls and patients with Alzheimer's disease. Black frames in the low-magnification images indicate the location of the high-magnification images to the right. Arrows indicate Aβ plaques, and arrowheads indicate the fibrinogen leakage and decreased Cldn5 and Glut1 in patients with Alzheimer's disease. Scale bar = 200 μm in A and B. Data are presented as mean ± SEM, n = 5, *P < 0.05, **P < 0.01.

APP/PS1 mice, a significant extravascular accumulation of fibrinogen was identified in the brain parenchyma (Fig. 2B and E), supporting BBB malfunction in the early stage of Alzheimer's disease pathology.

To determine whether BBB malfunction is associated with impaired BECs, we evaluated expression of tight junction protein Claudin-5 and glucose transporter Glut-1 both being essential for maintaining BEC integrity and function.⁴⁷

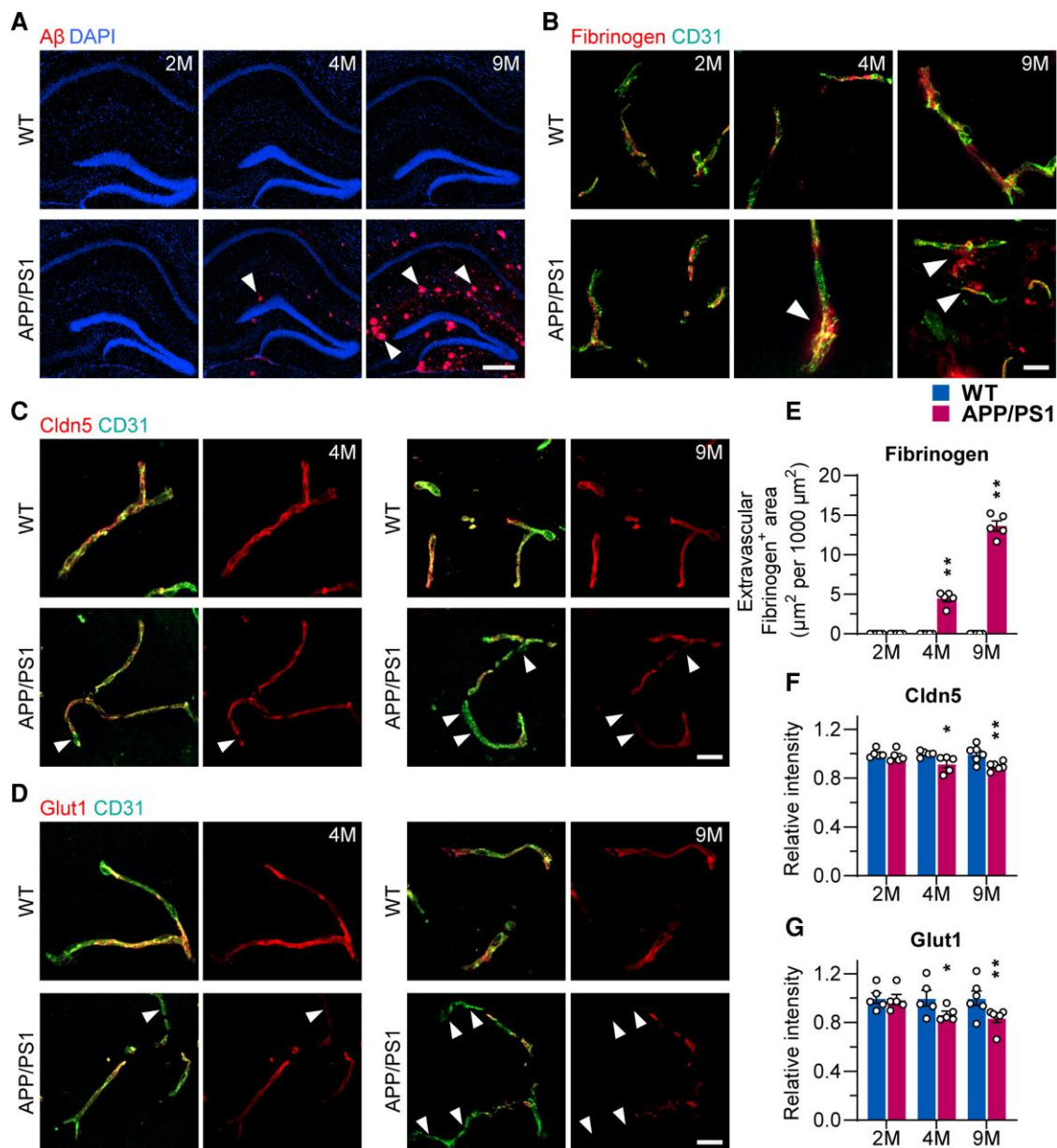


Figure 2 BBB dysfunction and BEC disruption presented at an early stage of Alzheimer's disease pathogenesis in APP/PS1 mice. (A) Immunostaining of A β in the hippocampus of 2-, 4- and 9-month-old wild-type (WT) and APP/PS1 mice (scale bar = 500 μ m). (B) Immunostaining of Fibrinogen and CD31 in the hippocampus of 2-, 4- and 9-month-old wild-type and APP/PS1 mice (scale bar = 20 μ m). (C) Immunostaining of Cldn5 in the hippocampus of 4- and 9-month wild-type and APP/PS1 mice (scale bar = 20 μ m). (D) Immunostaining of Glut1 in the hippocampus of 4- and 9-month-old wild-type and APP/PS1 mice (scale bar = 20 μ m). Arrowheads indicate the markers of interest in APP/PS1 mice. (E–G) Quantification of Fibrinogen, Cldn5 and Glut1 in the hippocampus of 2-, 4- and 9-month-old wild-type and APP/PS1 mice. Data are presented as mean \pm SEM, $n = 5$, * $P < 0.05$, ** $P < 0.01$.

We found that expression of Claudin-5 and Glut-1 were significantly decreased in APP/PS1 mice at 4 and 9 months compared to age-matched wild-type mice (both markers $P < 0.05$ and $P < 0.01$, respectively, Fig. 2C, D, F and G), consistent with fibrinogen leakage.

Collectively, our results obtained in patients with Alzheimer's disease and APP/PS1 mouse model indicate that BBB malfunction in Alzheimer's disease is linked to BEC impairment. In particular, the data obtained in APP/PS1 mice confirm this event occurs at the early stages of Alzheimer's disease pathology.

Decreased Wnt/ β -catenin signalling in cerebral microvessels of APP/PS1 mice

To identify which Wnt pathway is dysregulated in the BECs in Alzheimer's disease, we isolated cerebral microvessels from mouse brains at different ages (Fig. 3A), as evidence suggests that cerebral microvessels can better capture the BBB features thus also enabling mechanistic studies by measuring mRNA and protein changes in tight junction proteins.⁴⁹ We found that $99.3 \pm 0.15\%$ of the cells in the isolated cerebral microvessels

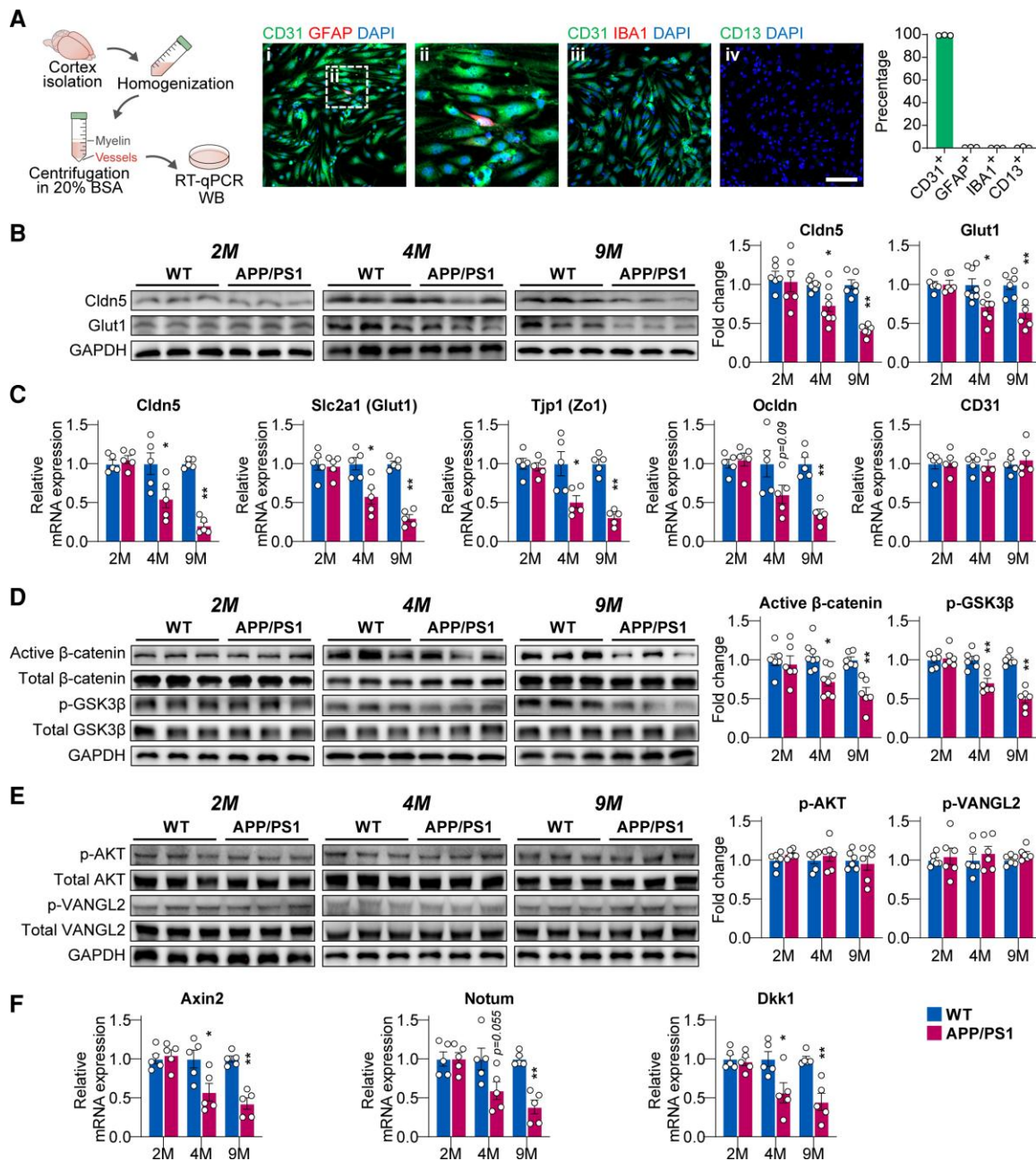


Figure 3 Decreased Wnt/β-catenin pathway in cerebral microvessels of APP/PS1 mice. (A) Schematic diagram of cerebral microvessels isolation. Representative immunostaining images of markers for (i and ii) endothelium (CD31), astrocyte (GFAP), (iii) microglia (IBA1) and (iv) pericyte (CD13) (scale bar = 100 μm). (B) Protein levels of Cldn5 and Glut1 in isolated cerebral microvessels of 2-, 4- and 9-month-old wild-type (WT) and APP/PS1 mice. (C) mRNA expression of Cldn5, Zo-1, Glut1, Ocldn and CD31 in microvessels from 2-, 4- and 9-month-old wild-type and APP/PS1 mice. (D) Protein levels of active β-catenin and phosphorylated Ser9-GSK3β in microvessels from 2-, 4- and 9-month-old wild-type and APP/PS1 mice. (E) Protein levels of AKT and Vangl2 in microvessels of 2-, 4- and 9-month-old wild-type and APP/PS1 mice. (F) mRNA expression of canonical Wnt pathway targets Axin2, Notum and DKK1 in microvessels of 2-, 4- and 9-month-old wild-type and APP/PS1 mice. Data are presented mean ± SEM, n = 6 in the 2- and 9-month group, n = 8 in the 4-month group for the western blot experiment; n = 5 for the RT-qPCR experiment; *P < 0.05, **P < 0.01.

were identified as CD31-positive BECs (Fig. 3A). Claudin-5 and Glut-1 protein, as well as their mRNA expression, in cerebral microvessels, were significantly decreased at 4 months of age (all P < 0.05 versus control) and further reduced at 9 months of age (all P < 0.01 versus control) in APP/PS1 mice (Fig. 3B). Similarly, mRNA expression of Zo-1 was also significantly reduced at 4 months of age (P < 0.05 versus control), and further reduced at 9 months of age (P < 0.01 versus control, Fig. 3C). Occludin mRNA

expression was only significantly reduced at 9 months (P < 0.01 versus control, Fig. 3C).

The phosphorylation status of the Wnt/β-catenin pathway-related markers, β-catenin and GSK3β, were significantly reduced in cerebral microvessels from APP/PS1 mice at 4 months (β-catenin P < 0.05, GSK3β P < 0.01 versus control) and 9 months (both β-catenin and GSK3β P < 0.01 versus control, Fig. 3D). However, phosphorylated AKT and Vangl2, essential for the PCP pathway activity,³⁷

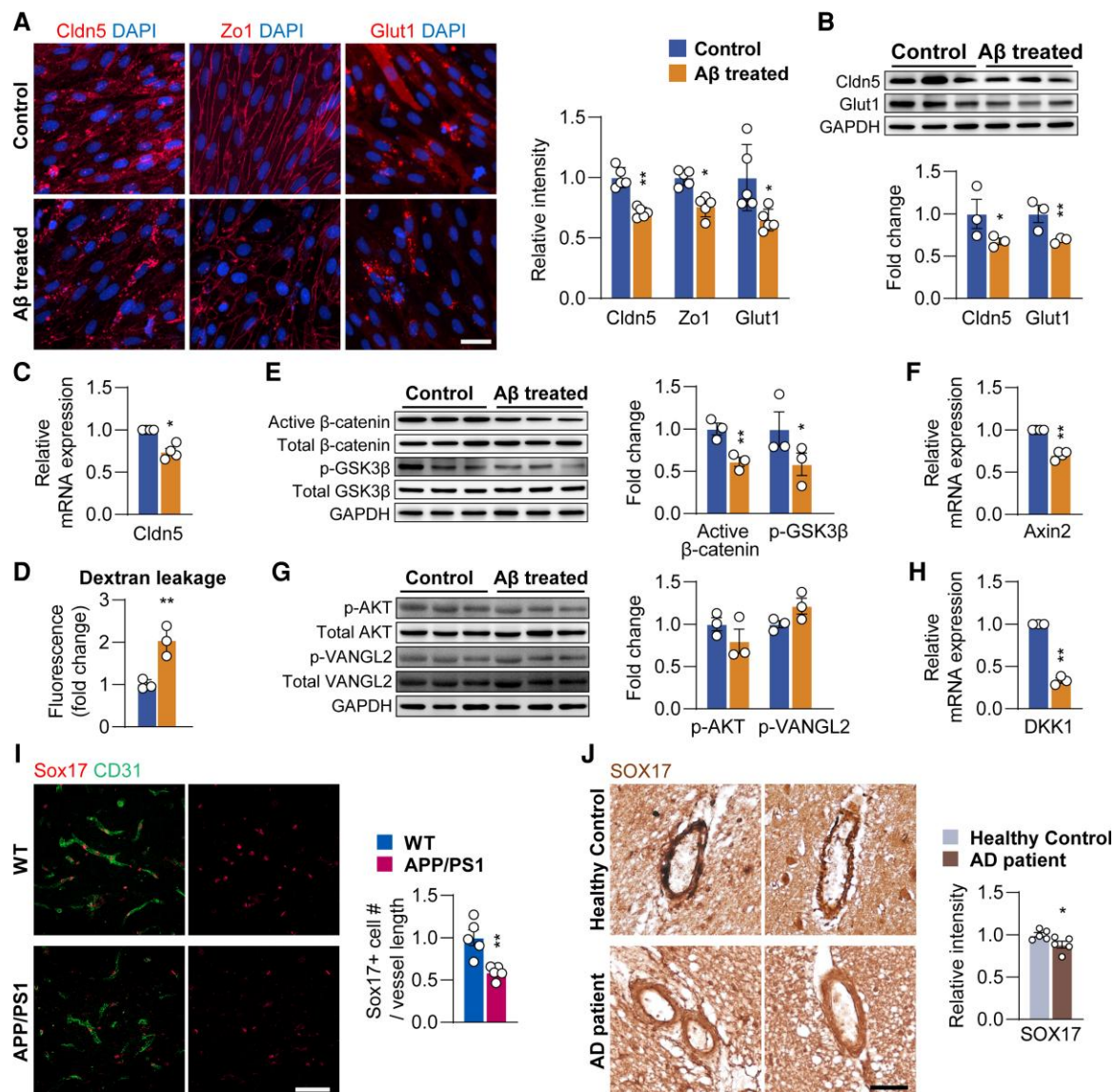


Figure 4 A β oligomer treatment induces BEC disruption and downregulates Wnt/ β -catenin signalling elements. (A) Immunostaining and quantification of Cldn5, Zo-1 and Glut1 in control and A β treated BECs (scale bar = 20 μ m). (B) Protein levels of Cldn5 and Glut1, (C) mRNA expression of *Cldn5*, (D) *in vitro* trans-well permeability assay, (E) protein levels of active β -catenin and phosphorylated Ser9-GSK3 β , (F) mRNA expression of *Axin2*, (G) protein levels of AKT and Vangl2 and (H) mRNA expression of *DKK1* in control and A β treated BECs. (I) Immunostaining and quantification of Sox17 in 4-month-old wild-type (WT) and APP/PS1 mice (scale bar = 50 μ m). (J) Sox17 levels in the cortex of health control and patients with Alzheimer's disease (scale bar = 50 μ m). Data are presented as mean \pm SEM, $n = 3$ in (B–H), $n = 5$ in (A, I and J), * $P < 0.05$, ** $P < 0.01$.

were not changed in the cerebral microvessels from APP/PS1 mice (Fig. 3E). Furthermore, reduced Wnt/ β -catenin signalling was also confirmed by the down-regulation of its downstream targets, *Axin2*, *Notum* and *DKK1* mRNA expression in the cerebral microvessels from APP/PS1 mice at 4 and 9 months of age (Fig. 3F).

Taken together, our results demonstrate that the AKT-independent Wnt/ β -catenin pathway (as opposed to the Wnt/PCP pathway) was suppressed in cerebral microvessels from APP/PS1 mice.

A β oligomer induces impairment of BECs and suppresses the Wnt/ β -catenin pathway

We observed BBB and BEC malfunction in 4-month old APP/PS1 mice when soluble A β oligomer begins to accumulate to form fibrillar A β

plaques.⁵⁰ As a result, we used primary rat BECs and A β_{25-35} fragments (toxic domain of the A β) to study A β oligomer-related toxicity in BECs.⁵¹ A β_{25-35} is the most cytotoxic component of senile plaques and is commonly used to establish the *in vitro* model of BBB malfunction.^{32–35,52} Although A β_{1-40} was also used to study BBB and cerebrovascular impairments in the literature, the A β_{1-40} has low-toxicity and even showed neuroprotective effects,^{53–55} hence we decided not to use it.

We used 20 μ M A β oligomer (A β_{25-35}) *in vitro*, because this concentration reduced Claudin-5 without affecting cell proliferation and viability (Supplementary Fig. 2). Exposing BECs to A β_{25-35} for 24 h resulted in a significant decrease in immunoreactivity for Claudin-5 ($P < 0.01$), Zo-1 ($P < 0.05$) and Glut-1 ($P < 0.05$, Fig. 4A). Changes in Claudin-5 ($P < 0.01$) and Glut-1 ($P < 0.05$) were further confirmed by western blotting (Fig. 4B). Reduction in Claudin-5

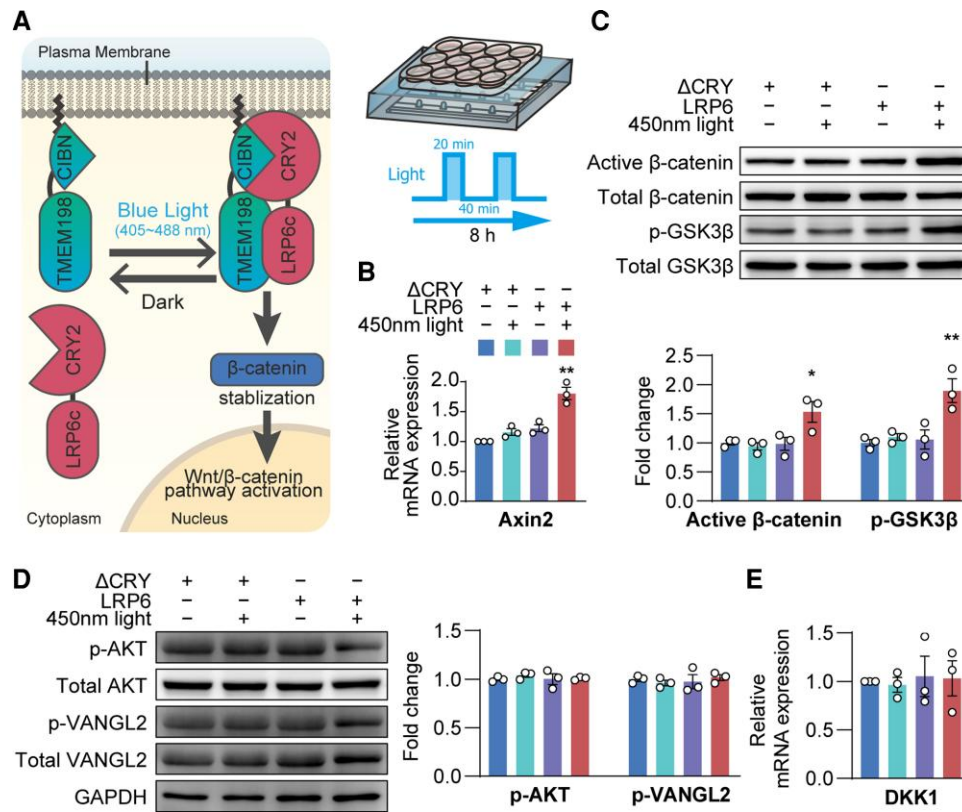


Figure 5 Optogenetic activation of Wnt/ β -catenin pathway. (A) Schematic diagram of the optogenetic method. (B) *Axin2* mRNA expression, (C) protein levels of active β -catenin and phosphorylated Ser9-GSK3 β , (D) protein level of AKT and Vangl2 and (E) *Dkk1* mRNA expression in the BECs. Data are presented as mean \pm SEM, $n = 3$, * $P < 0.05$, ** $P < 0.01$.

was also observed at the mRNA level ($P < 0.05$, Fig. 4C). $A\beta_{25-35}$ induced reduction in barrier integrity of BECs was accessed by the permeability assay (Fig. 4D).

Furthermore, $38.8 \pm 5.5\%$ reduction in active β -catenin ($P < 0.01$), $41.6 \pm 13.3\%$ reduction in phosphorylated Ser9-GSK3 β ($P < 0.05$, Fig. 4E) and $29.8 \pm 2.5\%$ reduction in *Axin2* mRNA expression ($P < 0.01$, Fig. 4F), were observed in $A\beta_{25-35}$ -treated BECs *in vitro*. Consistent with the *in vivo* results, AKT and Vangl2 activities in BECs were not affected by $A\beta_{25-35}$ treatment (Fig. 4G), suggesting a specific suppression of the Wnt/ β -catenin pathway only in BECs. However, *Dkk1* mRNA level was reduced after $A\beta_{25-35}$ treatment ($P < 0.01$, Fig. 4H), which may be an adaptive change to the suppressed Wnt/ β -catenin signalling.

To further confirm the suppressed Wnt/ β -catenin pathway signalling in BECs in Alzheimer's disease, the downstream target of Wnt/ β -catenin pathway, sex determining region Y-box 17 (Sox17), was quantified. Immunostaining of Sox17 was reduced in the cerebral vessels from both APP/PS1 mice ($P < 0.01$, Fig. 4I) and patients with Alzheimer's disease ($P < 0.05$, Fig. 4J).

Taken together, our results indicate that $A\beta_{25-35}$ suppressed Wnt/ β -catenin activity by reducing BEC markers critical for BBB integrity; the Wnt/ β -catenin therefore may be a potential new treatment target.

Optogenetic activation of Wnt/ β -catenin pathway signalling

To achieve a precise regulation of Wnt/ β -catenin pathway, we used an opsin-free optogenetics tool. Opsin-free optogenetics allows

light-mediated modulation of the intracellular signalling pathways in live cells with high temporal and spatial accuracy.^{42,56–59} Here, we used an in-house developed optogenetic tool (OptoLRP6).⁴⁰ As shown in Fig. 5A, under blue-light stimulation, the CRY2-CIBN association allows the interaction between LRP6 and transmembrane protein 198 (TMEM198) to specifically activate LRP6-Wnt signalling.⁶⁰ This results in a reversible activation of the Wnt/ β -catenin pathway. Based on our preliminary experiments, the light cycling was set to a 20 min on and 40 min off mode for maximum light-exposure efficacy and preservation of cell viability.

After light exposure for 8 h, *Axin2* mRNA expression ($P < 0.01$, Fig. 5B), active β -catenin ($P < 0.05$, Fig. 5C) and phosphorylated Ser9-GSK3 β ($P < 0.01$, Fig. 5C) were all increased in light-stimulated OptoLRP6-infected BECs compared with control Δ CRY plasmid-transfected BECs. However, AKT and Vangl2 activities, as well as *Dkk1* mRNA level, remained unchanged, confirming that targeting OptoLRP6 exclusively activates the Wnt/ β -catenin pathway, but not the Wnt/PCP pathway.

Light-induced OptoLRP6 activation rescued $A\beta_{25-35}$ -induced BEC impairment

We then treated OptoLRP6 or control Δ CRY plasmid-transfected BECs with $A\beta_{25-35}$ for 24 h, followed by light exposure for 8 h (Fig. 6A). After light stimulation, *Axin2* level in the $A\beta_{25-35}$ treated OptoLRP6-transfected group was the highest ($P < 0.01$ versus all other three groups, Fig. 6B). The suppressed immunoreactivities of Claudin-5, Zo-1 and Glut-1 were significantly recovered by light stimulation in the OptoLRP6 group after the exposure to

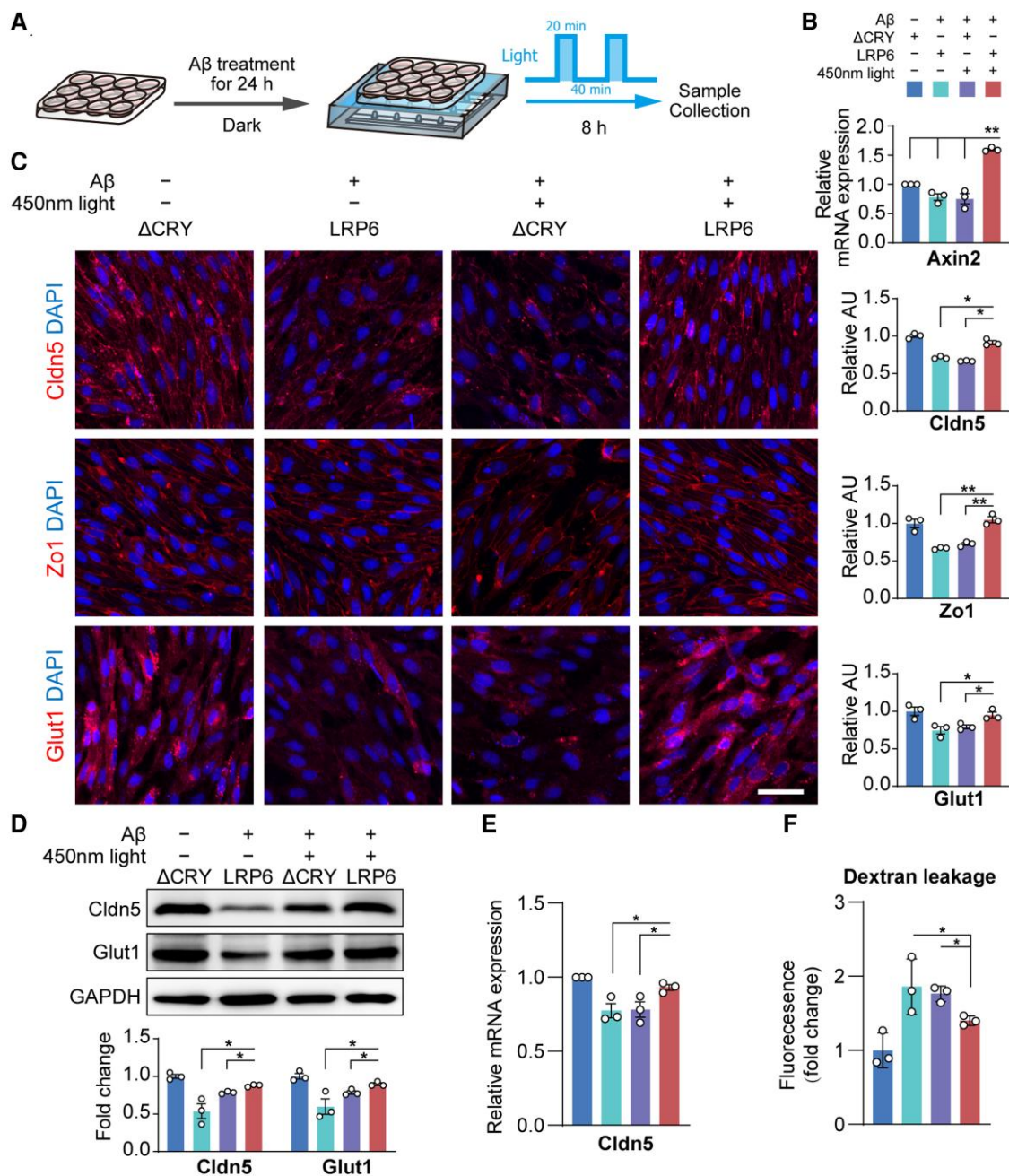


Figure 6 Light-stimulated OptoLRP6 activation rescues BEC disruption after A β oligomer treatment. (A) Schematic diagram of experiment design. (B) Axin2 mRNA expression, (C) immunostaining and quantification of Cldn5, Zo-1 and Glut1 (scale bar = 20 μ m), (D) protein levels of Cldn5 and Glut1, (E) Cldn5 mRNA expression and (F) *in vitro* trans-well permeability assay in BECs. Data are presented as mean \pm SEM, $n=3$, * $P < 0.05$, ** $P < 0.01$.

A β_{25-35} (Fig. 6C), consistent with the results of Wnt ligand Wnt3a treatment (Supplementary Fig. 3). Changes in Claudin-5 were confirmed by both western blotting (Fig. 6D) and qPCR (Fig. 6E), while changes in Glut-1 were confirmed by western blotting (Fig. 6D). The dye-tracers experiment confirmed the improvement of BBB permeability in BECs transfected with OptoLRP6 and illuminated (Fig. 6F). The results indicate that the activation of the Wnt/ β -catenin pathway by targeting LRP6 has the potential therapeutic value to rescue A β -induced BBB malfunction in Alzheimer's disease.

Preactivation of the Wnt/ β -catenin pathway by OptoLRP6 prevents A β_{25-35} -induced BEC disruption

BECs impairment at an early stage of Alzheimer's disease pathology in APP/PS1 mice suggests that BBB malfunction may contribute to Alzheimer's disease pathogenesis. Therefore, we investigated whether preactivation of the Wnt/ β -catenin pathway can prevent A β -induced BEC impairments. Primary BECs transfected with OptoLRP6 or control Δ CRY plasmid were stimulated by blue light for 8 h, followed by exposure to A β_{25-35} for 24 h (Fig. 7A).

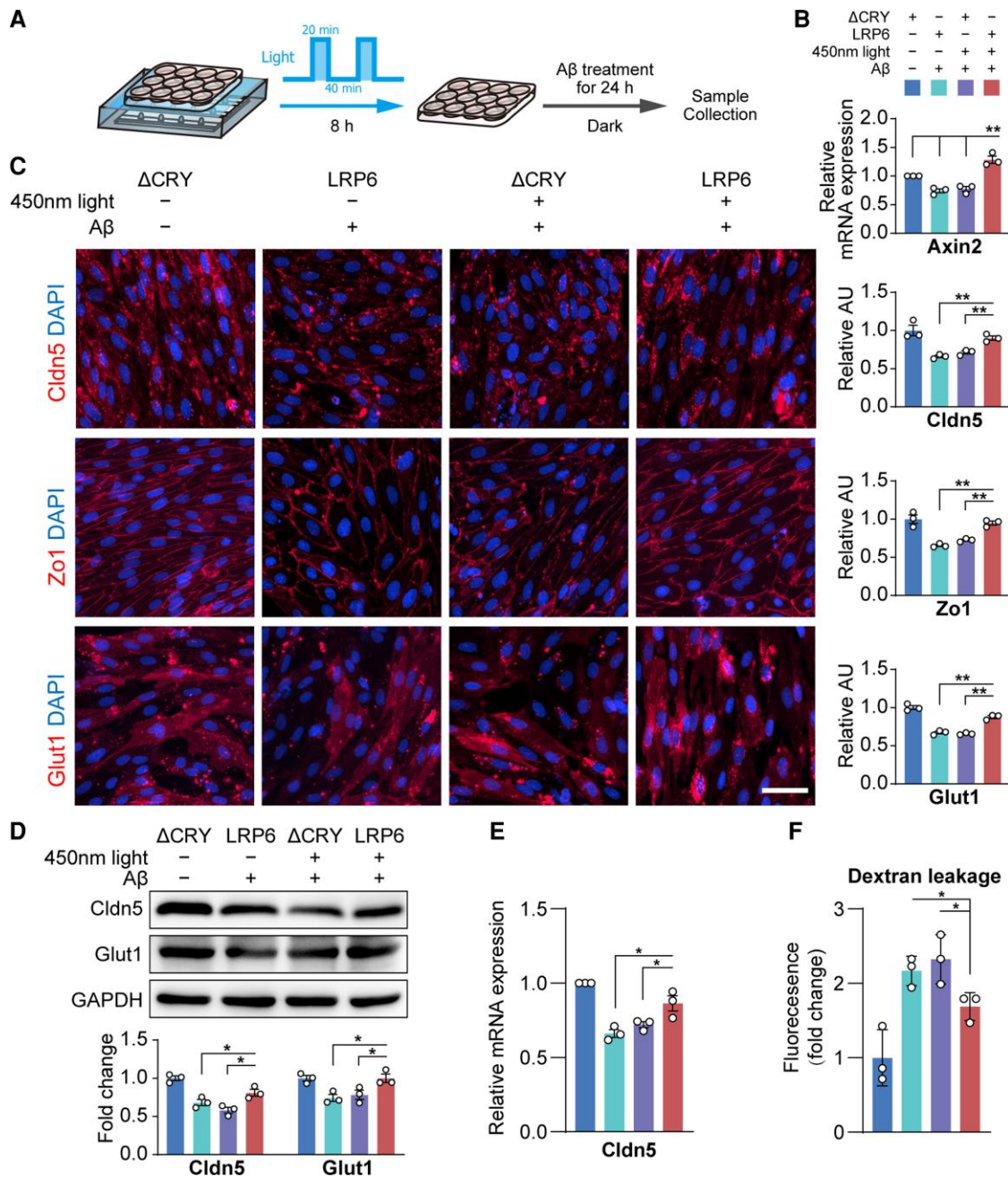


Figure 7 Activation of the Wnt/β-catenin pathway by OptoLRP6 prevents Aβ oligomer-induced BEC disruption. (A) Schematic diagram of experiment design. (B) Axin2 mRNA expression, (C) immunostaining and quantification of Cldn5, Zo-1 and Glut1 (scale bar = 20 μm), (D) protein levels of Cldn5 and Glut1, (E) Cldn5 mRNA expression and (F) *in vitro* trans-well permeability assay in BECs. Data are presented as mean ± SEM, n = 3, *P < 0.05, **P < 0.01.

Axin2 levels were significantly increased in BECs transfected with OptoLRP6 after light and Aβ_{25–35} exposure as compared to all the other ΔCRY groups (all P < 0.01, Fig. 7B). The protein levels of tight junction proteins Claudin-5, Zo-1 and glucose transporter Glut-1 in BECs transfected with OptoLRP6 were nearly the same as controls (Fig. 7C–E), in line with the results of Wnt ligand Wnt3a treatment (Supplementary Fig. 3). The dye-tracers experiment also confirmed the improvement of BBB permeability *in vitro* (Fig. 7F). These data indicate the preventive effects of activated Wnt/β-catenin signalling against Aβ_{25–35}-induced BEC dysfunction.

Discussion

This study confirmed that BBB malfunction caused by impaired BECs plays a key role in the early stage of Alzheimer's disease pathophysiology.^{8–12,61,62} By using both human Alzheimer's disease specimens and APP/PS1 mice, we found that BBB damage stemmed from reduced levels of tight junction proteins and glucose transporter Glut-1. Dysregulation of Wnt/β-catenin pathway signalling in cerebral microvessels by Aβ oligomer may be the underlying mechanism of BEC impairment in Alzheimer's disease. Using a novel optogenetic tool, we discovered a promising new target for

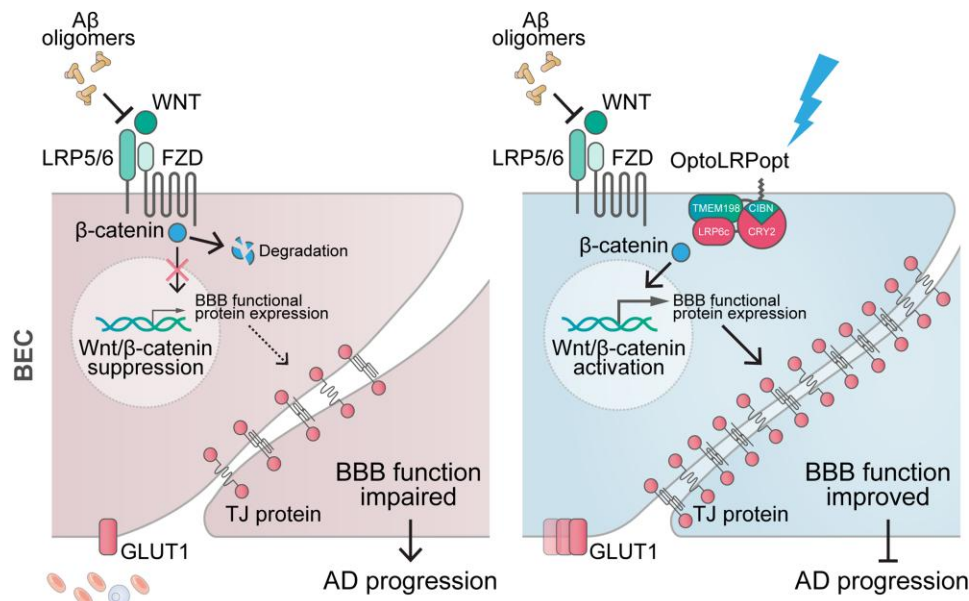


Figure 8 Targeting LRP6 in the Wnt/ β -catenin pathway in BECs alleviates BBB dysfunction. In the Alzheimer's disease (AD) brain, A β oligomers suppress Wnt/ β -catenin signalling in the BECs, leading to reduced expression of endothelial functional proteins and BBB malfunction. Our recently developed optogenetic tool allows precise regulation of LRP6, the upstream regulator of Wnt/ β -catenin signalling. The activation of Wnt/ β -catenin signalling restored A β -inhibited BEC function by reversing and preventing A β -induced BEC pathological changes.

treatment strategies, the Wnt coreceptor LRP6, which can effectively activate Wnt/ β -catenin pathway to protect BECs against A β_{25-35} -induced toxicity and restore BEC abnormalities in Alzheimer's disease (Fig. 8).

It is widely acknowledged that BBB malfunction contributes to many neuropathologies,^{47,63,64} although there are still inconsistencies in showing the extravasation of plasma-derived proteins.^{8,21–25,43–45} Nonetheless, leakage of blood protein fibrinogen into perivascular tissue following the breakdown of BBB is increasingly recognized as a contributor to neuropathology.⁶⁵ Deploying neuroprotectant to rescue behavioural deficits in Alzheimer's disease model simultaneously improved BBB and cerebrovascular integrity, along with reduced A β formation.⁶⁶ However, it is difficult to determine whether the vascular protection was primary or secondary to reduced A β accumulation. In the present study, we showed that BBB integrity is impaired in Alzheimer's disease patients and APP/PS1 mice, as indicated by increased levels of plasma-derived fibrinogen in extravascular tissues and decreased levels of BEC tight junction proteins and Glut-1. In particular, our data in APP/PS1 mice confirm that this sign occurs at the early stages of Alzheimer's disease. This suggests that fibrinogen may be used as a new imaging biomarker of dysfunctional BECs and BBB in humans, and/or early diagnosis of Alzheimer's disease. However, as the information on familial or sporadic Alzheimer's disease was not registered at the Brain Bank, it remains unclear which specific Alzheimer's disease type was investigated.

BEC-related pathologies occur in the early stages of Alzheimer's disease. Thus, it is natural to ask the question of whether targeting repair of BECs can protect BBB function and thereafter prevent/reverse the decline of the Alzheimer's disease brain. To better understand the mechanisms that impair BECs in Alzheimer's disease, Wnt pathway was studied because of its involvement in BEC pathologies^{26,28,29} and association with risk factors of Alzheimer's disease, such as LRP6, GSK3 β , Dkk1 and Vangl2.^{67,68} In the brains of both patients with Alzheimer's disease and APP/PS1 mice, we discovered a significant reduction in Wnt/ β -catenin pathway activity,

mostly driven by the suppressed upstream regulator LRP6. Other regulators, such as GSK3 β and AKT, as well as Wnt/PCP pathway, did not seem to be involved. Moreover, we demonstrate that A β_{25-35} induced BBB dysfunction and BEC disruption through suppressing the canonical Wnt/ β -catenin pathway signalling.²⁶ This effect may be mediated by A β_{25-35} binding to Frizzled receptors, which are required to activate the Wnt/ β -catenin pathway by LRP6,³⁵ while we can exclude AKT signalling and the non-canonical Wnt/PCP pathway. In addition, we found a significant decrease in Dkk1 in BECs in APP/PS1 mice, contrary to previously reported increases in Dkk1 in neurons,^{32,69} with the underlying mechanism still unknown. Nevertheless, our findings provide a plausible mechanism of the pathogenesis of BBB and BEC dysfunction in Alzheimer's disease brains, which may exacerbate Alzheimer's disease neuropathology.^{70,71} Protecting or reversing vascular function may slow down the decline or preserve neurological function.

To determine whether Wnt/ β -catenin pathway, particularly its upstream regulator LRP6, is a valid target to protect cerebrovascular function, we adopted a novel optogenetic technique to accurately regulate LRP6 on the cell surface to activate Wnt/ β -catenin pathway signalling, since the Wnt ligand is unable to target the canonical Wnt/ β -catenin pathway exclusively.⁷² LRP6 has been linked to synaptic and cognitive abnormalities in aged mice and patients with Alzheimer's disease.^{31,73} Curcumin, a natural compound, has been demonstrated to increase LRP6 levels to exert potential neuroprotective effects in several Alzheimer's disease animal models^{74–76}; however, it is not suitable for Alzheimer's disease treatment due to its low bioavailability. In this study, using our optogenetic tool, we showed that increasing the Wnt/ β -catenin signalling by activating LRP6 partially restored expression of tight junction proteins Claudin-5, Zo-1 and glucose transporter Glut-1 after A β_{25-35} exposure, suggesting such approach may be used as a potential therapeutic strategy to alleviate or even reverse A β_{25-35} -induced BBB malfunction in patients with Alzheimer's disease. Furthermore, activation of Wnt/ β -catenin pathway signalling can

also prevent pathological changes in BECs induced by A β_{25-35} exposure, suggesting the potential for LRP6 as a preventive treatment to protect BBB function in Alzheimer's disease. However, whether targeting LRP6 can also reduce/clear A β accumulation and preserve neurological function needs to be examined in future in APP/PS1 mice at different ages.

In conclusion, BBB dysfunction due to BECs disruption is present in human Alzheimer's disease brains, and occurs at the early stages of Alzheimer's disease pathogenesis in APP/PS1 mice. In BECs, targeting the Wnt/ β -catenin pathway upstream coreceptor LRP6 can restore the A β oligomer-induced pathologies, suggesting LRP6 as a new potential target for Alzheimer's disease treatment.

Funding

This study was supported by grants from the National Natural Science Foundation of China (NSFC 81971309, 32170980, 32070964, 31871045), National Key Research and Development Program of China (2017YFA0106000, 2021ZD0201703), Guangdong Basic and Applied Basic Research Foundation (2022B1515020012, 2019A1515011333) and Shenzhen Fundamental Research Program (RCYX20200714114644167, JCYJ20210324123212035, JCYJ20190809161405495).

Competing interests

The authors report no competing interests.

Supplementary material

Supplementary material is available at *Brain* online.

References

- Kraepelin E. *Psychiatrie; ein Lehrbuch für Studierende und Ärzte*. vol 2. Barth; 1910.
- De Strooper B, Karran E. The cellular phase of Alzheimer's disease. *Cell*. 2016;164:603–615.
- Liu PP, Xie Y, Meng XY, Kang JS. History and progress of hypotheses and clinical trials for Alzheimer's disease. *Signal Transduct Target Ther*. 2019;4:29.
- Long JM, Holtzman DM. Alzheimer Disease: an update on pathobiology and treatment strategies. *Cell*. 2019;179:312–339.
- Guo T, Zhang D, Zeng Y, Huang TY, Xu H, Zhao Y. Molecular and cellular mechanisms underlying the pathogenesis of Alzheimer's disease. *Mol Neurodegener*. 2020;15:40.
- Huang J, Shen M, Qin X, Wu M, Liang S, Huang Y. Acupuncture for the treatment of Alzheimer's disease: An overview of systematic reviews. *Front Aging Neurosci*. 2020;12:574023.
- Tolar M, Abushakra S, Sabbagh M. The path forward in Alzheimer's disease therapeutics: Reevaluating the amyloid cascade hypothesis. *Alzheimers Dement*. 2020;16:1553–1560.
- Montagne A, Barnes SR, Sweeney MD, et al. Blood-brain barrier breakdown in the aging human hippocampus. *Neuron*. 2015;85:296–302.
- Yamazaki Y, Kanekiyo T. Blood-brain barrier dysfunction and the pathogenesis of Alzheimer's disease. *Int J Mol Sci*. 2017;18:1965.
- van de Haar HJ, Burgmans S, Jansen JF, et al. Blood-brain barrier leakage in patients with early Alzheimer disease. *Radiology*. 2016;281:527–535.
- Nation DA, Sweeney MD, Montagne A, et al. Blood-brain barrier breakdown is an early biomarker of human cognitive dysfunction. *Nat Med*. 2019;25:270–276.
- Montagne A, Nation DA, Sagare AP, et al. APOE4 Leads to blood-brain barrier dysfunction predicting cognitive decline. *Nature*. 2020;581:71–76.
- Langen UH, Ayloo S, Gu C. Development and cell biology of the blood-brain barrier. *Annu Rev Cell Dev Biol*. 2019;35:591–613.
- Huang Z, Wong LW, Su Y, et al. Blood-brain barrier integrity in the pathogenesis of Alzheimer's disease. *Front Neuroendocrinol*. 2020;59:100857.
- Profaci CP, Munji RN, Pulido RS, Daneman R. The blood-brain barrier in health and disease: important unanswered questions. *J Exp Med*. 2020;217:e20190062.
- Kadry H, Noorani B, Cucullo L. A blood-brain barrier overview on structure, function, impairment, and biomarkers of integrity. *Fluids Barriers CNS*. 2020;17:69.
- Bauer HC, Krizbai IA, Bauer H, Traweger A. 'You shall not pass'-tight junctions of the blood brain barrier. *Front Neurosci*. 2014;8:392.
- Morita K, Sasaki H, Furuse M, Tsukita S. Endothelial claudin: Claudin-5/TMVCF constitutes tight junction strands in endothelial cells. *J Cell Biol*. 1999;147:185–194.
- Tornavaca O, Chia M, Dufton N, et al. ZO-1 controls endothelial adherens junctions, cell-cell tension, angiogenesis, and barrier formation. *J Cell Biol*. 2015;208:821–838.
- Winkler EA, Nishida Y, Sagare AP, et al. GLUT1 Reductions exacerbate Alzheimer's disease vasculo-neuronal dysfunction and degeneration. *Nat Neurosci*. 2015;18:521–530.
- Wisniewski HM, Kozlowski PB. Evidence for blood-brain barrier changes in senile dementia of the Alzheimer type (SDAT). *Ann N Y Acad Sci*. 1982;396:119–129.
- Slemmon JR, Hughes CM, Campbell GA, Flood DG. Increased levels of hemoglobin-derived and other peptides in Alzheimer's disease cerebellum. *J Neurosci*. 1994;14:2225–2235.
- Zipser BD, Johanson CE, Gonzalez L, et al. Microvascular injury and blood-brain barrier leakage in Alzheimer's disease. *Neurobiol Aging*. 2007;28:977–986.
- Alafuzoff I, Adolfsson R, Grundke-Iqbal I, Winblad B. Blood-brain barrier in Alzheimer dementia and in non-demented elderly. An immunocytochemical study. *Acta Neuropathol*. 1987;73:160–166.
- Tomimoto H, Akiyoshi I, Suenaga T, et al. Alterations of the blood-brain barrier and glial cells in white-matter lesions in cerebrovascular and Alzheimer's disease patients. *Stroke*. 1996;27:2069–2074.
- Liebner S, Corada M, Bangsow T, et al. Wnt/ β -catenin signaling controls development of the blood-brain barrier. *J Cell Biol*. 2008;183:409–417.
- Komiya Y, Habas R. Wnt signal transduction pathways. *Organogenesis*. 2008;4:68–75.
- Laksitorini MD, Yathindranath V, Xiong W, Hombach-Klonisch S, Miller DW. Modulation of wnt/ β -catenin signaling promotes blood-brain barrier phenotype in cultured brain endothelial cells. *Sci Rep*. 2019;9:19718.
- Niu J, Tsai HH, Hoi KK, et al. Aberrant oligodendroglial-vascular interactions disrupt the blood-brain barrier, triggering CNS inflammation. *Nat Neurosci*. 2019;22:709–718.
- Artus C, Glacial F, Ganeshamoorthy K, et al. The Wnt/planar cell polarity signaling pathway contributes to the integrity of tight junctions in brain endothelial cells. *J Cereb Blood Flow Metab*. 2014;34:433–440.
- Liu CC, Tsai CW, Deak F, et al. Deficiency in LRP6-mediated Wnt signaling contributes to synaptic abnormalities and amyloid pathology in Alzheimer's disease. *Neuron*. 2014;84:63–77.

32. Elliott C, Rojo AI, Ribe E, et al. A role for APP in Wnt signalling links synapse loss with beta-amyloid production. *Transl Psychiatry*. 2018;8:179.
33. De Ferrari GV, Inestrosa NC. Wnt signaling function in Alzheimer's disease. *Brain Res Rev*. 2000;33:1–12.
34. Garrido JL, Godoy JA, Alvarez A, Bronfman M, Inestrosa NC. Protein kinase C inhibits amyloid beta peptide neurotoxicity by acting on members of the Wnt pathway. *FASEB J*. 2002;16:1982–1984.
35. Magdesian MH, Carvalho MM, Mendes FA, et al. Amyloid-beta binds to the extracellular cysteine-rich domain of frizzled and inhibits Wnt/beta-catenin signaling. *J Biol Chem*. 2008;283:9359–9368.
36. Park KS, Lee RD, Kang SK, et al. Neuronal differentiation of embryonic midbrain cells by upregulation of peroxisome proliferator-activated receptor-gamma via the JNK-dependent pathway. *Exp Cell Res*. 2004;297:424–433.
37. Yue X, Lan F, Yang W, et al. Interruption of beta-catenin suppresses the EGFR pathway by blocking multiple oncogenic targets in human glioma cells. *Brain Res*. 2010;1366:27–37.
38. Sellers KJ, Elliott C, Jackson J, et al. Amyloid beta synaptotoxicity is Wnt-PCP dependent and blocked by fasudil. *Alzheimers Dement*. 2018;14:306–317.
39. Mao B, Wu W, Li Y, et al. LDL-receptor-related protein 6 is a receptor for dickkopf proteins. *Nature*. 2001;411:321–325.
40. Krishnamurthy VV, Hwang H, Fu J, Yang J, Zhang K. Optogenetic control of the canonical Wnt signaling pathway during xenopus laevis embryonic development. *J Mol Biol*. 2021;433:167050.
41. Millucci L, Raggiaschi R, Franceschini D, Terstappen G, Santucci A. Rapid aggregation and assembly in aqueous solution of A beta (25–35) peptide. *J Biosci*. 2009;34:293–303.
42. Su Y, Huang X, Huang Z, et al. Early but not delayed optogenetic RAF activation promotes astrocytogenesis in mouse neural progenitors. *J Mol Biol*. 2020;432:4358–4368.
43. Schlageter NL, Carson RE, Rapoport SI. Examination of blood-brain barrier permeability in dementia of the Alzheimer type with [^{68}Ga]EDTA and positron emission tomography. *J Cereb Blood Flow Metab*. 1987;7:1–8.
44. Dysken MW, Nelson MJ, Hoover KM, Kuskowski M, McGeachie R. Rapid dynamic CT scanning in primary degenerative dementia and age-matched controls. *Biol Psychiatry*. 1990;28:425–434.
45. Caserta MT, Caccioppo D, Lapin GD, Ragin A, Groothuis DR. Blood-brain barrier integrity in Alzheimer's disease patients and elderly control subjects. *J Neuropsychiatry Clin Neurosci*. 1998;10:78–84.
46. Obermeier B, Daneman R, Ransohoff RM. Development, maintenance and disruption of the blood-brain barrier. *Nat Med*. 2013;19:1584–1596.
47. Zlokovic BV. The blood-brain barrier in health and chronic neurodegenerative disorders. *Neuron*. 2008;57:178–201.
48. Montagne A, Zhao Z, Zlokovic BV. Alzheimer's disease: A matter of blood-brain barrier dysfunction? *J Exp Med*. 2017;214:3151–3169.
49. Navone SE, Marfia G, Invernici G, et al. Isolation and expansion of human and mouse brain microvascular endothelial cells. *Nat Protoc*. 2013;8:1680–1693.
50. Larson ME, Lesne SE. Soluble abeta oligomer production and toxicity. *J Neurochem*. 2012;120(Suppl 1):125–139.
51. Millucci L, Ghezzi L, Bernardini G, Santucci A. Conformations and biological activities of amyloid beta peptide 25–35. *Curr Protein Pept Sci*. 2010;11:54–67.
52. Cuevas E, Rosas-Hernandez H, Burks SM, et al. Amyloid beta 25–35 induces blood-brain barrier disruption in vitro. *Metab Brain Dis*. 2019;34:1365–1374.
53. Zou K, Kim D, Kakio A, et al. Amyloid beta-protein (abeta)1–40 protects neurons from damage induced by Abeta1–42 in culture and in rat brain. *J Neurochem*. 2003;87:609–619.
54. Merino-Zamorano C, Fernandez-de Retana S, Montanola A, et al. Modulation of amyloid-beta1–40 transport by ApoA1 and ApoJ across an in vitro model of the blood-brain barrier. *J Alzheimers Dis*. 2016;53:677–691.
55. Wang D, Chen F, Han Z, Yin Z, Ge X, Lei P. Relationship between amyloid-beta deposition and blood-brain barrier dysfunction in Alzheimer's disease. *Front Cell Neurosci*. 2021;15:695479.
56. Tischer D, Weiner OD. Illuminating cell signalling with optogenetic tools. *Nat Rev Mol Cell Biol*. 2014;15:551–558.
57. Zhang K, Cui B. Optogenetic control of intracellular signaling pathways. *Trends Biotechnol*. 2015;33:92–100.
58. Huang T, Zhang Y, Wang Z, et al. Optogenetically controlled TrkA activity improves the regenerative capacity of hair-follicle-derived stem cells to differentiate into neurons and glia. *Adv Bio (Weinh)*. 2020;5:e2000134.
59. Shin G, Gomez AM, Al-Hasani R, et al. Flexible near-field wireless optoelectronics as subdermal implants for broad applications in optogenetics. *Neuron*. 2017;93:509–521.e3.
60. Liang J, Fu Y, Cruciat CM, et al. Transmembrane protein 198 promotes LRP6 phosphorylation and Wnt signaling activation. *Mol Cell Biol*. 2011;31:2577–2590.
61. Kalaria RN, Hedera P. Differential degeneration of the cerebral microvasculature in Alzheimer's disease. *Neuroreport*. 1995;6:477–480.
62. Zenaro E, Piacentino G, Constantin G. The blood-brain barrier in Alzheimer's disease. *Neurobiol Dis*. 2017;107:41–56.
63. Erickson MA, Banks WA. Blood-brain barrier dysfunction as a cause and consequence of Alzheimer's disease. *J Cereb Blood Flow Metab*. 2013;33:1500–1513.
64. Sweeney MD, Zhao Z, Montagne A, Nelson AR, Zlokovic BV. Blood-brain barrier: From physiology to disease and back. *Physiol Rev*. 2019;99:21–78.
65. Petersen MA, Ryu JK, Akassoglou K. Fibrinogen in neurological diseases: Mechanisms, imaging and therapeutics. *Nat Rev Neurosci*. 2018;19:283–301.
66. Lazic D, Sagare AP, Nikolakopoulou AM, Griffin JH, Vassar R, Zlokovic BV. 3K3A-activated Protein C blocks amyloidogenic BACE1 pathway and improves functional outcome in mice. *J Exp Med*. 2019;216:279–293.
67. Kibar Z, Vogan KJ, Groulx N, Justice MJ, Underhill DA, Gros P. Ltap, a mammalian homolog of drosophila strabismus/Van Gogh, is altered in the mouse neural tube mutant loop-tail. *Nat Genet*. 2001;28:251–255.
68. Rao TP, Kuhl M. An updated overview on Wnt signaling pathways: A prelude for more. *Circ Res*. 2010;106:1798–1806.
69. Killick R, Ribe EM, Al-Shawi R, et al. Clusterin regulates beta-amyloid toxicity via dickkopf-1-driven induction of the wnt-PCP-JNK pathway. *Mol Psychiatry*. 2014;19:88–98.
70. Bhat RV, Andersson U, Andersson S, Knerr L, Bauer U, Sundgren-Andersson AK. The conundrum of GSK3 inhibitors: Is it the dawn of a new beginning? *J Alzheimers Dis*. 2018;64:S547–S554.
71. Athar T, Al Balushi K, Khan SA. Recent advances on drug development and emerging therapeutic agents for Alzheimer's disease. *Mol Biol Rep*. 2021;48:5629–5645.
72. Samarzija I, Sini P, Schlange T, Macdonald G, Hynes NE. Wnt3a regulates proliferation and migration of HUVEC via canonical and non-canonical Wnt signaling pathways. *Biochem Biophys Res Commun*. 2009;386:449–454.
73. Alarcon MA, Medina MA, Hu Q, et al. A novel functional low-density lipoprotein receptor-related protein 6 gene alternative splice

- variant is associated with Alzheimer's disease. *Neurobiol Aging*. 2013;34:1709.e9-18.
74. Tiwari SK, Agarwal S, Seth B, et al. Curcumin-loaded nanoparticles potently induce adult neurogenesis and reverse cognitive deficits in Alzheimer's disease model via canonical Wnt/beta-catenin pathway. *ACS Nano*. 2014;8:76–103.
75. Farkhondeh T, Samarghandian S, Pourbagher-Shahri AM, Sedaghat M. The impact of curcumin and its modified formulations on Alzheimer's disease. *J Cell Physiol*. 2019;234:16953–16965.
76. Sanei M, Saberi-Demneh A. Effect of curcumin on memory impairment: a systematic review. *Phytomedicine*. 2019;52:98–106.